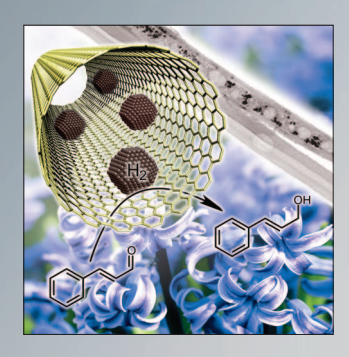
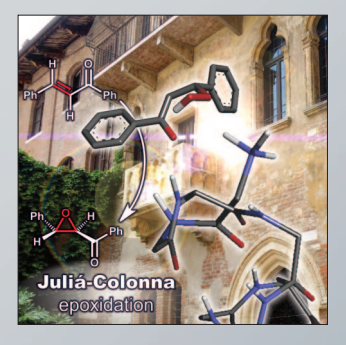
Heterogeneous & Homogeneous & Bio-

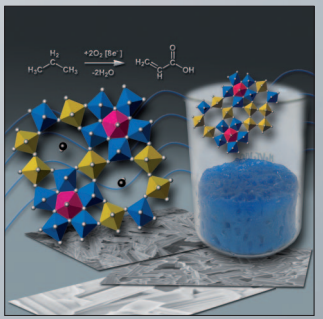
CHEMCATCHEM

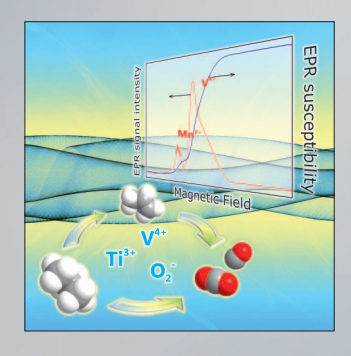
CATALYSIS

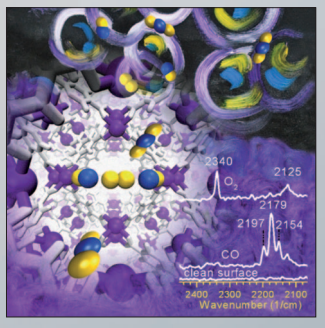




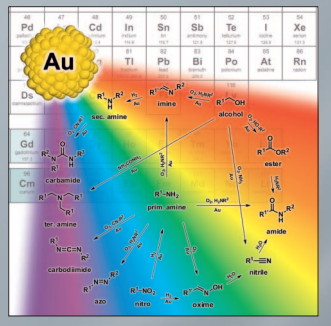




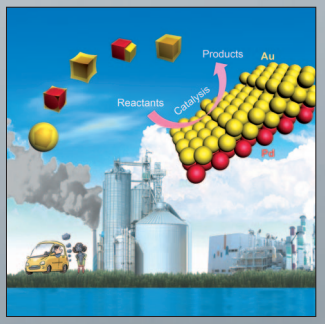


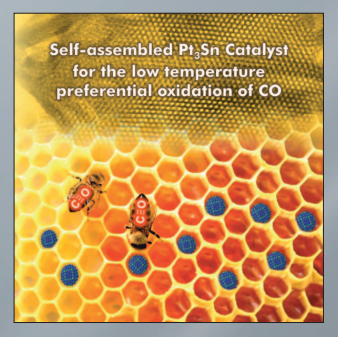
















Europe

Reprint

© Wiley-VCH Verlag GmbH & Co. KGaA, Weinheim

WILEY-VCH





Heterogeneous & Homogeneous & Bio-

CHEMCATCHEM

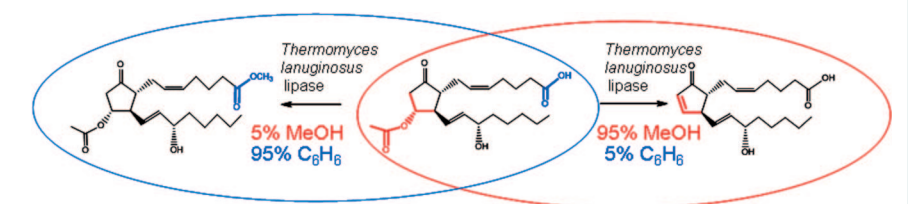
CATALYSIS

Table of Contents

L. Villo,* A. Metsala, S. Tamp, J. Parve, I. Vallikivi, I. Järving, N. Samel, Ü. Lille, T. Pehk, O. Parve

1998 - 2010

Thermomyces lanuginosus Lipase with Closed Lid Catalyzes Elimination of Acetic Acid from 11-Acetyl-Prostaglandin E₂



Methanol makes the difference: Thermomyces lanuginosus lipase (TLL) may catalyze either esterification or elimination of 11-acetyl-prostaglandin E2 in methanol-containing reaction medium.

An increase in the methanol concentration in benzene from 5% to 95% leads to the exclusive switch of reactions from esterification to elimination.



DOI: 10.1002/cctc.201400019

Thermomyces lanuginosus Lipase with Closed Lid Catalyzes Elimination of Acetic Acid from 11-Acetyl-Prostaglandin E₂

Ly Villo,*[a] Andrus Metsala,[a] Sven Tamp,[a] Jaan Parve,[b] Imre Vallikivi,[c] Ivar Järving,[a] Nigulas Samel, [a] Ülo Lille, [a] Tõnis Pehk, [d] and Omar Parve [a]

A lipase may catalyze either one or more of the three reactions of 11-acetyl-prostaglandin E₂ in methanol-containing reaction medium: esterification, deacetylation, and/or elimination. The catalytic performance depends on the lipase and on the methanol content. An increase in the methanol concentration in benzene from 5% to 95% leads to the exclusive switch of reactions from esterification to elimination catalyzed by Thermomyces lanuginosus lipase (TLL). To explain the switch, molecular dynamics simulations of solvation of TLL in benzene and in

methanol were performed. Solvation in methanol leads to the closing of the lid. The repositioning of the oxyanion hole towards the catalytic triad blocks the catalysis of ester synthesis whereas enabling TLL to act as an acetyl-β-ketol eliminase. In benzene the lid is open, allowing esterification to occur. Docking analysis of 11-acetyl-prostaglandin E2 into the active site of the solvated TLL structures suggested the occurrence of reactions in accordance with the experiment.

Introduction

Developing methods for the synthesis of novel prostaglandin (PG) analogues has been in focus owing to the ongoing characterization of PG receptors. [1] Derivatives of PGA2 (3) have been found in high concentration in a soft coral Plexaura homomalla.[2,3] The formation of PGA2 derivatives in corals from PGE₂ through esterase-catalyzed reactions has previously been proposed. [4] Several putative therapeutic applications of A-type prostaglandins have been highlighted, [5-9] and among others a mediating role of PGA_2 in cellular arrest and death, which is important for cancer research.[10-12] As semisynthesis is the most economical approach for the preparation of less accessible prostanoids for medical research, PGA2 has been used as a starting material for the synthesis of novel PGA2 derivatives.[13] Lipase-catalyzed reactions have been useful in the field of semisynthesis of prostanoids^[14-16] as well as for the separation of prostanoid stereoisomers. [17-20]

[a] Dr. L. Villo, Dr. A. Metsala, Dr. S. Tamp, Dr. I. Järving, Prof. N. Samel, Prof. Ü. Lille, Dr. O. Parve Department of Chemistry, Tallinn University of Technology. Ehitajate tee 5, 19086 Tallinn (Estonia) Fax: (+37)26202828E-mail: lee@chemnet.ee

[b] I. Parve Institute of Technology University of Tartu Nooruse 1, 50411 Tartu (Estonia)

[c] Dr. I. Vallikivi TRD-Riodiscovery Tiigi 61b, 50410 Tartu (Estonia)

National Institute of Chemical Physics and Biophysics Akadeemia tee 23, 12618 Tallinn (Estonia)

Supporting information for this article is available on the WWW under http://dx.doi.org/10.1002/cctc.201400019.

Lipases catalyze the hydrolysis of triglycerides in emulsions, activated by contact with water/triglyceride interface, which causes the relocation of the lid of the active site. For Thermomyces lanuginosus lipase (TLL), one of the lid's amino acid residues is also a constituent part of the oxyanion hole that stabilizes oxyanionic tetrahedral intermediates. Opening of the lid induces, therefore, the optimal spatial position of the catalytic triad and of the oxyanion hole residues, required for the catalytic activation of a lipase.^[21]

Lipases have different lid types, ranging from complex structures to having no lid at all.[22] Despite the fact that TLL has a short lid of simple structure, there is still no existing unequivocal understanding of the structure of the lid of TLL. Different researchers define it with variations as consisting of the following amino acid residues: either of 85-93, [23] 82-96, [24] or of 82-90.[22] In this work the definition of 82-96 residues has been preferred, because Trp89 would obviously be considered to belong to the central part of the lid, and Ser83 has to be involved.[21]

Lipases can be activated in a hydrophobic organic solvent in the same manner as at the water/triglyceride interface. [25,26] Lipases are less active in water-miscible solvents, and they are almost deactivated regarding the catalysis of acyl-transfer reactions in shorter alcohols like methanol and ethanol; however, exceptions have been observed.[27] Lipases are used to catalyze methanolysis (for example in biodiesel production)^[28-31] and, in addition, to usual acyl transfer reactions, they have been shown to catalyze aldol condensation^[32] and hemiacetal opening/hydroxyaldehyde acylation. [33]

Molecular dynamics (MD) simulations of tetrahedral intermediates with following trajectory analysis have been the methodological strategy used in molecular modeling studies of lipase-catalyzed acyl-transfer reactions.^[34] Regioselectivity of the lipase-catalyzed acetylation of isomeric prostaglandins of F type has been investigated by using this approach. [35] Characteristics allowing to prognosticate regioselectivity quite precisely are: 1) root mean square deviation (RMSD) of the enzyme geometry along the MD simulation trajectory and 2) energy of the function-based subset of the tetrahedral intermediate.[36]

However, the above mentioned strategy cannot be used for modeling of lipase-catalyzed reactions occurring according to a mechanism devoid of the covalent bonding of the substrate to the enzyme. This is the case in the elimination of acetic acid from 11 Ac-PGE₂ (1) catalyzed by TLL—an abnormal catalytic performance discovered by our group^[1,15]—further demonstrating the intriguing promiscuity of lipases (Scheme 1). For

Scheme 1. Using different content of methanol in the reaction medium alters exclusively the catalytic performance of TLL in methanolysis of 11 Ac-PGE, (1).

the modeling of the reactions of this type, analysis of the docking sites and modes has to be undertaken to explain the feasibility of a certain reaction or selectivity observed. For instance, the regioselectivity of the lipase-catalyzed acylation of flavonoid glycosides has been prognosticated by means of docking.[37]

MD simulation studies of lipase solvation in organic solvents[38,39] as well as in water have given useful information about conformational changes depending on medium[40,41] and, in particular, about lid opening in hydrophobic solvents and closing in water. [24] MD simulations have also been performed to explore substrate binding by the enzyme. [23,42] Solvation of lipases may have a dramatic influence on the activity and stereoselectivity of a lipase. [43]

However, several reported MD simulation studies tend to suffer from the lack of a clearly defined particular catalytic effect observed experimentally for the lipase under study, which could allow verification of the corresponding modeling results more precisely. In this regard, the results of our current study will provide more clarity and details useful to the field of lipase modeling.

The intrigue of the current paper has arisen from the empirical results^[15,16] according to which TLL catalyzes the synthesis of 11 Ac-PGE₂ methyl ester (2) in benzene with low methanol content (95:5) (Scheme 1), whereas the same enzyme catalyzes the elimination of acetic acid from the same substrate in a solvent system qualitatively the same, differing only by an opposite ratio of the components (C₆H₆/CH₃OH 5:95).^[1,15] The elimination mechanism has previously been expected to involve the generation and stabilization of the corresponding enolate by the lipase. [15] Modeling results on a related process catalyzed by ketosteroid isomerase^[44] and also the discovery of a similar novel enzymatic acetylation-elimination process have been reported.[45]

Our objective herein is to explain the structural reason behind the dramatic switch of reactions catalyzed by TLL dependent on the ratio of solvents in a system consisting of the same components. Particular steps taken to achieve this goal were: 1) preparation, by means of MD simulation, of virtual structures of TLL solvated in both, methanol and benzene; 2) performing the docking analysis of the substrate 11 Ac-PGE₂ (1) into the active site of solvated TLL structures to identify which of the reactions is suggested by the geometry of the docking poses.

Results and Discussion

The MD simulation of TLL in solvent boxes filled with benzene and methanol, respectively, (and for comparison in vacuum) was performed. Changes in the conformation and hydration of TLL structure along the MD simulation trajectory were characterized and analyzed. On the one hand, solvation of TLL in benzene can be assumed to lead to conservation of the solvated structure and on the other hand, methanol can be expected to dehydrate the enzyme, leading to a more significant modification of the enzyme conformation. To prepare the enzyme for MD simulation studies, a preliminary relaxation of the enzyme/solvent system by means of MD simulation for 2 ns was performed. However, by inspection of, firstly, the evolution of the interatomic distance plots and, secondly, the progress of the RMSD of the TLL geometry, it became evident that the initial relaxation/equilibration phase of MD simulation may last longer than 2 ns for the solvation of TLL. This was further evaluated statistically by calculating the average RMSD as well as the average interatomic distances of the active site for different parts of the MD simulation trajectory. Based on these results, it was concluded that for the systems under study the initial relaxation/equilibration phase may probably last up to 10 ns in addition to the preliminary 2 ns of the MD simulation. Taking into account this conclusion and also some diverging MD indications, the multiple solvated TLL structures were taken arbitrarily from MD simulation trajectories and used for docking studies to provide an independent verification that no inferences would be drawn by using solvated structures of TLL taken from the part of the MD simulation trajectory corresponding to the initial relaxation phase of MD simulation. For instance, docking of 11 Ac-PGE₂ into the TLL structure solvated in benzene for 3 ns (of MD) yields qualifying docking complexes that suggest the occurrence of all three reactions: esterification, deacetylation and elimination which is not in accordance with the experiment. However, it should be mentioned that the scoring (the binding energy) suggests the preference of the esterification. On the contrary, the use of the TLL solvated structures taken from the 11 ns time point of the MD in benzene versus methanol yield exclusively the docking complexes that suggest the occurrence of the esterification and elimination reactions, respectively, in accordance with the experimental results as well as with the geometrical considerations drawn from studies of the corresponding solvated structures. These results confirm that the part of the MD simulation trajectory beginning at least from 10-11 ns evidently corresponds to the equilibrated production phase of the simulation from which inferences may be drawn relating to the "wet" experimental state.

The docking targets, structures of solvated TLL, are characterized separately by their interatomic distances (Figures 1 and 2, Table 1). Docking of 11 Ac-PGE2 into the active site of TLL molecule with the geometry that corresponds to a solvated structure (solvent molecules were removed prior to docking) was performed within a docking cell (see the Supporting Information, Table S3). All docking complexes that meet the respective qualification criteria based on interatomic distances were identified and are presented in Table 5, together with their scoring results. The qualification criteria characterize the molecular recognition mode that refers to the ability of solvated TLL to catalyze any of the three above-mentioned reactions.

Synthetic experiments were performed by using NMR analysis of the reaction mixtures for an estimation of the reaction

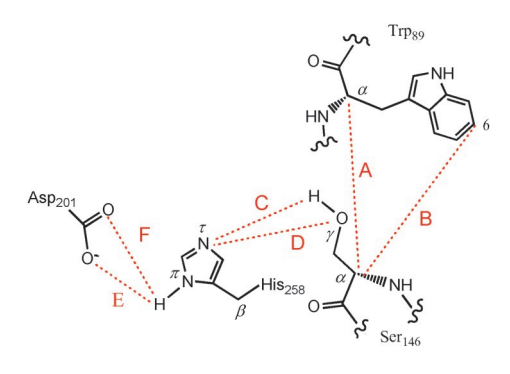


Figure 1. Distances between the atoms of the residues Asp201, His258, and Ser146 of the catalytic triad of TLL and the central residue of the lid, Trp89 and their designation as A-F.

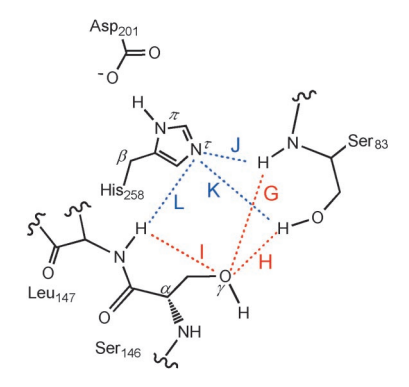


Figure 2. Distances G. H. and I are the distances between the O^{γ} atom of Ser146 of the catalytic triad and three hydrogen atoms of the oxy-anion hole, respectively; distances J. K. and L are the distances between the N^t atom of His258 of the catalytic triad and the three hydrogen atoms, respectively.

Table 1. The interatomic distances characterizing the solvated TLL docking structures taken from 3, 7, 11, 15 ns and the structure corresponding to the minimum energy, compared to MD input structures and the structures obtained by MD in vacuum. The distances characterize the position of the central part of the lid (A, B) and the shift of the oxyanion hole (G-L) versus the catalytic triad, respectively, and the position of the constituents of the catalytic triad (C-F).

Simulation	Interatomic distances [Å] ^[a]											
time [ns]	Α	В	C	D	E	F	G	Н	I	J	K	L
	Solvent: I	methanol										
O ^[c]	11.70	8.04	1.85	2.80	2.47	1.74	3.1	4.0	1.6	5.7	6.9	5.6
3	10.02	9.0	2.13	3.06	2.43	1.98	2.4	3.8	3.9	5.5	5.7	5.7
7	11.91	14.0	1.90	2.82	2.12	2.05	2.2	3.9	3.8	4.9	4.8	5.3
11	11.64	12.14	1.95	2.87	2.80	1.92	1.9	4.0	3.7	4.7	5.1	5.3
15	11.54	14.14	4.39	4.42	2.23	2.01	2.1	3.6	1.9	5.0	4.3	5.7
min. energy structure ^[b]	10.36	7.64	3.43	3.88	2.60	1.78	2.8	3.6	2.0	5.7	6.9	5.7
	Solvent: l	benzene										
O ^[c]	11.44	8.23	1.82	2.76	2.42	1.79	4.6	4.3	2.5	6.9	6.8	5.2
3	13.16	9.38	2.29	3.12	1.99	4.05	4.7	4.4	2.3	7.4	7.6	5.2
7	12.79	19.12	1.94	2.84	1.73	3.86	5.3	4.3	2.9	7.1	6.5	5.5
11	12.76	18.40	2.31	3.25	1.80	3.95	4.7	4.4	2.6	7.2	7.3	5.7
15	12.84	18.29	1.86	2.83	1.75	3.77	4.7	4.7	2.8	7.2	7.2	5.6
min. energy structure ^[b]	11.81	8.42	1.88	2.84	1.83	2.44	4.5	4.3	2.4	6.9	6.8	5.2
	In vacuo											
O ^[c]	11.12	7.53	1.75	2.71	2.69	1.80						
3	10.41	7.78	4.05	3.93	2.24	2.17						
7	9.03	5.13	4.97	4.79	2.35	2.03						

[a] Distances A-F correspond to the ones in Figure 1, distances G-L correspond to the ones in Figure 2; [b] the TLL geometry from MD trajectory identified as corresponding to minimum potential energy structure; [c] input structures of TLL corresponding to the starting point of MD simulation at 0.0 ns.

selectivities and the initial velocities dependent on lipases and methanol concentration.

MD simulation of TLL solvation; changes in the geometry of the enzyme active site

The reposition of the following particular constituents of the enzyme (Figures 1 and 2) was analyzed along the MD simulation trajectory, and results are listed in Tables 1 and 2: 1) the center of the lid, Trp89, versus Ser146 of the catalytic triad; 2) the components of the catalytic triad versus each other; and 3) the oxyanion hole (consisting of NH and OH hydrogen atoms of Leu147 and Ser83, the latter is also a constituent part of the lid) versus the components of the catalytic triad, and the oxy-anion hole backbone N-atom of Ser83 towards the catalytic triad Ser146 backbone C^{α} -atom (distance M, see Table 2).

Spatial position of the lid

Tracking of the distances A and B (Figure 3, Table 1) and also of the distances G, H, and M (Figure 4, Tables 1 and 2) leads to the conclusion that in benzene the lid of the active site of TLL is open, whereas in methanol it is closed. For instance, the distance B describing the position of the Trp89 bicyclic fragment in relation to Ser146 is 12.1 Å in methanol and 18.4 Å in benzene, in both cases found for 11 ns TLL structures that represent considerably well the "wet" structures as has been determined further by docking of the substrate (see Table 5).

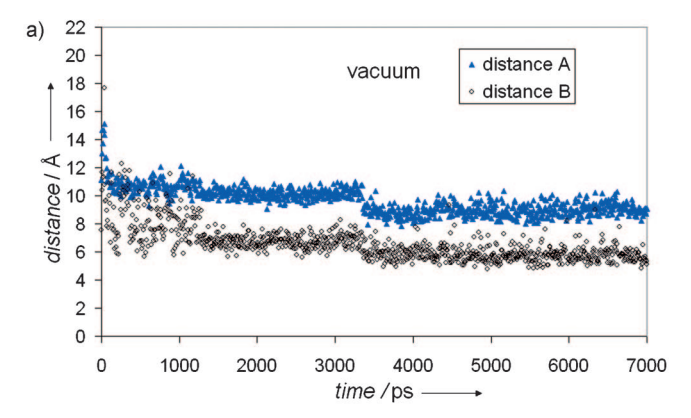
A more remarkable indication of the lid closing is the repositioning of the lid hinge Ser83 backbone (distance M; Table 2) for 2 Å towards Ser146 C^{α} atom, because the relative change of the distance is large. This large distance change is an indication that the lid hinge has turned. Consequently, Ser83 NH hydrogen atom of the oxyanion hole has shifted towards O^{γ} of Ser146 (Figure 2, Table 1) to form a tight H-bond.

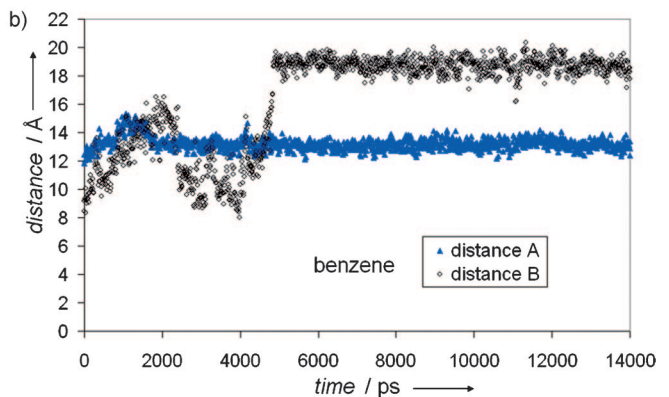
Position of the catalytic triad constituents and the lid

Regarding the catalytic triad, the distances E and F (Figure 1) characterizing the position of the oxygen atoms of the side

Table 2. Distance M characterizing the movement of the TLL lid/oxyanion hole backbone N-atom of Ser83 (of the "lid hinge" region) towards the catalytic triad Ser146 backbone C^{α} -atom in different solvents.

Simulation	Distance M	[Å]
time [ns]	methanol	benzene
3	4.94	7.16
7	4.75	6.82
11	4.64	6.56
15	4.97	6.53





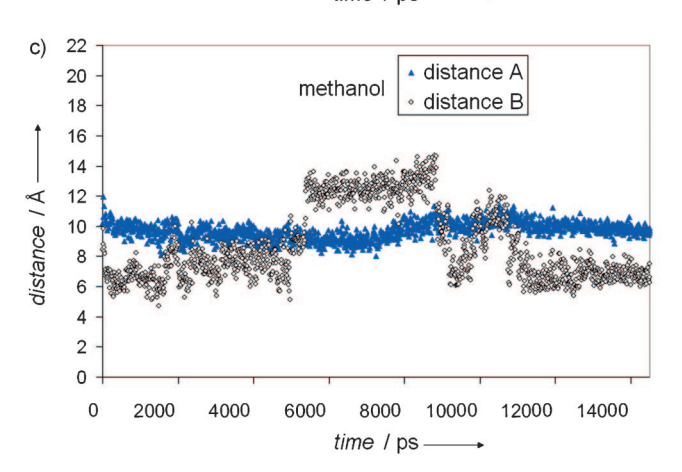


Figure 3. Plots of the interatomic distances A and B (see Figure 1) from MD simulation trajectories of TLL in a) vacuum and in solvent boxes filled with b) methanol and c) benzene as a function of time demonstrating the movement of the central region of the lid.

chain carboxyl group of Asp201 are almost equal in methanol but clearly distinguished in benzene (Table 1, Supporting Information Figure S1a). The distances between atoms of Ser146 OH group and His258 N^T (C and D,) are short (2 and 3 Å, respectively) and stable in benzene. In methanol, the distances C and D are short (2 and 3 Å, respectively) and relatively stable until their behavior changes sharply beginning from 14 ns, and these distances become larger and labile (3-6 Å). The latter effect indicates that a change of the lid conformation beginning from 14 ns takes place in methanol; this can also be seen from the tracking of the distance M (Table 2), which becomes

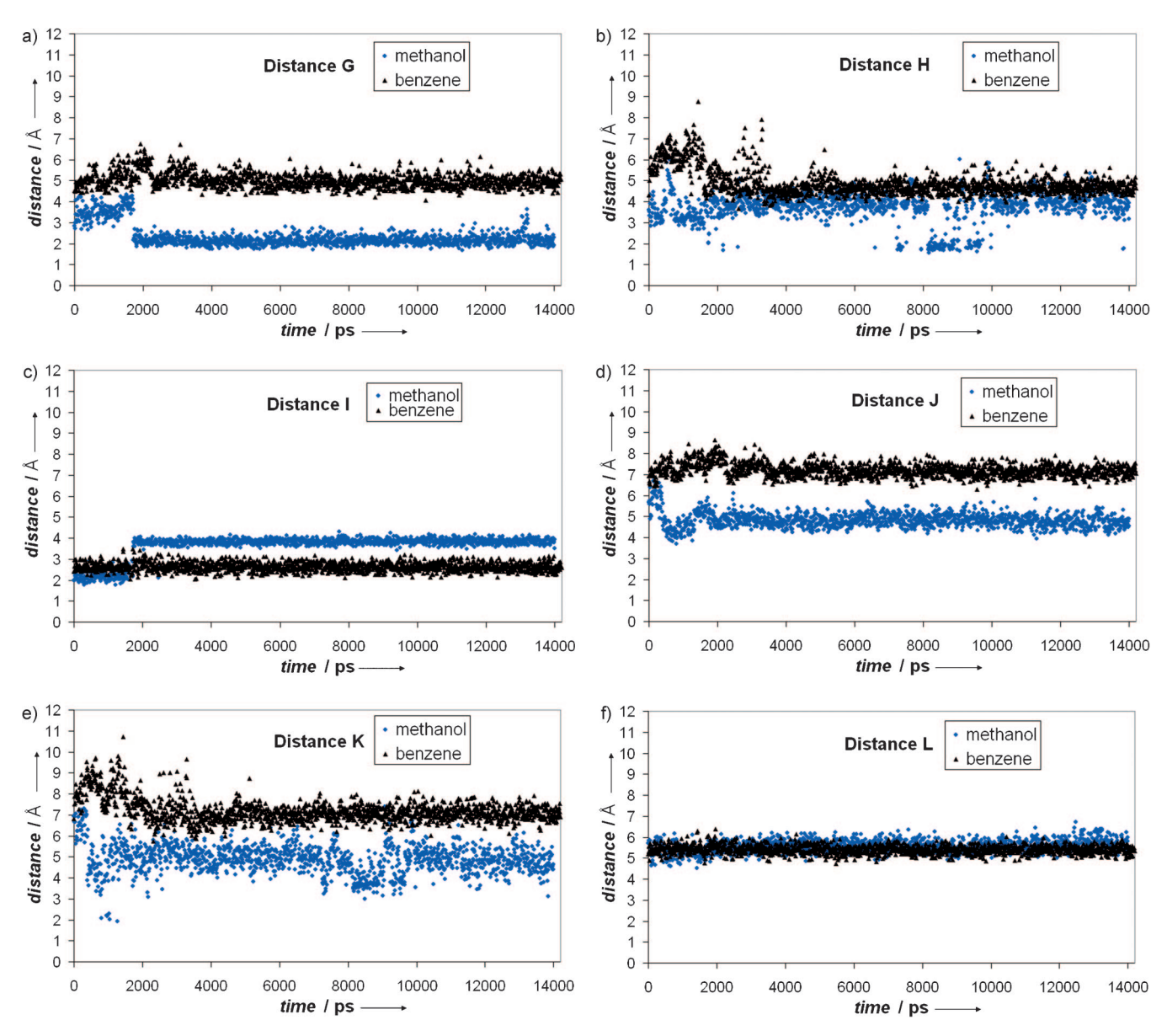


Figure 4. Plots of interatomic distances G, H, I, J, K, and L (Figure 2) from MD simulation trajectories of TLL in solvent boxes filled with methanol and benzene as a function of time demonstrating the distance changes of the nucleophilic O^{γ} atom of Ser146 and three hydrogen atoms of the oxyanion hole (distances G, H, I) and of the N^t atom of His258 and the above three hydrogen atoms of the oxyanion hole (distances J, K, L), respectively.

0.4-0.5 Å longer; the lid backbone removes itself from the catalytic triad Ser146 backbone C^α atom for this distance. However, the length G of the hydrogen bond between Ser146 O^{γ} and Ser83 NH hydrogen atom remains stable during all of the MD simulation for 40 ns (see Table 3); the average distance G found for the different parts of the MD simulation trajectory is approximately 2.1 Å (Table 3). Consequently, the lid of TLL is closed during all of the MD simulation in methanol, the change of the lid conformation at 14 ns is only a negligible correction of the lid geometry and the structural reasons for anomalous catalytic performance do not change in essence during MD.

Shift of the oxyanion hole

Inspection of the distances G, J, and K in benzene and in methanol, respectively for the TLL structures at 11 ns indicates that they are (respectively) 2.8, 2.5, and 2.2 Å shorter (Table 1) in methanol than in benzene. This proves clearly that the shift of the oxyanion hole towards the catalytic triad has taken place in methanol. As a result, Ser83 NH hydrogen atom forms tight H bond (G=1.9 Å) with the Ser146 O^{γ} atom (in addition, the backbone hinders O^{γ} sterically), thus greatly reducing its nucleophilicity and consequently the ability to catalyze acyl transfer reactions. Importantly, the plots (Figure 4) reveal that the change of the distances G, H, I, J, and K, which characterize the position of the oxyanion hole/lid hinge along the MD simulation trajectory, stabilizes during 2-4 ns of the MD simulation

Table 3. MD simulation of TLL solvation in benzene and methanol: average RMSD of the backbone C^{α} atoms and the interatomic distances M and G characterizing the mutual position of Ser146 of the catalytic triad and Ser83 of the oxyanion hole.

MD simulation		Solvent					
trajectory subdivisions		Benzene			Methanol		
(time) [ps]	RMSD [Å]	M [Å]	G [Å]	RMSD [Å]	M [Å]	G [Å]	
0–1990	1.38	6.93	5.18	1.43	5.18	2.14	
2000–3990	1.48	7.01	5.25	1.66	4.88	2.12	
4000–5990	1.55	6.76	4.98	1.79	4.89	2.08	
6000–7990	1.55	6.75	4.95	1.86	4.93	2.11	
8000–9990	1.58	6.79	4.95	1.83	4.95	2.12	
10 000-11 990	1.59	6.76	4.94	1.99	4.93	2.06	
12000-13990	1.61	6.76	4.95	1.96	4.95	2.12	
14000-18990				1.89	5.32	2.09	
19000-23990				1.90	5.53	2.10	
24000-28990				1.99	5.37	2.07	
29 000-33 990				1.91	5.48	2.09	
34000-39990				1.96	5.44	2.10	

(in addition to the preliminary relaxation during 2 ns). The change of the distance A, which characterizes the repositioning of the backbone of the central part of the lid, behaves in an analogous manner (Figure 3). The average distances M and G (Table 3) calculated for the different parts of the MD simulation trajectories confirm clearly that the lid backbone of TLL moves brusquely causing the shift of the oxyanion hole already during the preliminary relaxation by MD for 2 ns in methanol.

Probable mechanism of the switch of the catalytic performance

The shortening of the distance M between the lid and the catalytic triad backbones of TLL in methanol versus benzene (Table 2) of 2 Å (at 11 ns) causes the simultaneous repositioning of the two hydrogen atoms of the oxyanion hole. They move from their initial distances (G and H) in benzene of 4-5 Å to O^Y atom of Ser146 (that obviously is a catalytically proper position for the stabilization of the oxyanionic tetrahedral intermediates) and from their distances (J and K) of approximately 7 Å to N^τ of His258 to the catalytically proper position at the distance of 4–5 Å to the His258 N^τ atom. Notably, to catalyze elimination, an oxyanionic enolate has to be stabilized by the lipase catalytic machinery, which is similar to the stabilization of the tetrahedral intermediate involved in the catalysis of the acyl-transfer reactions. The shift of the oxyanion hole to the proper distance probably enables His258 imidazole to act further as an efficient "proton shuttle" (see Figure 8) in generating the enolate of the substrate and the transfer of the abstracted proton to the leaving acetate group in catalyzing the elimination of acetic acid from the acetyl-β-ketol moiety of 11 Ac-PGE₂ (2).

Minimum energy structures

It can be concluded from the interatomic distances presented in Table 1 and Table 2 that TLL structures solvated in benzene and methanol, respectively, differ strongly from each other and also from those obtained by MD simulation in vacuum. Regarding the minimum energy TLL solvated structures obtained from the MD simulation trajectories, they differ only slightly, in terms of the interatomic distances of the active site, from the MD input structures and probably do not represent the equilibrated phase of the MD simulations. This conclusion was additionally verified by docking of the substrate to the minimum energy structures to disprove suggestions to use these structures for docking studies (see diverging results in Table 5). It should be noted in

advance that docking of the substrate $11\,\text{Ac-PGE}_2$ to the TLL solvated structures taken from 11 ns of the both MD simulation trajectories has given results in exclusive accordance with the experimental results.

The molecular dynamics of TLL in methanol were simulated as long as 40 ns (Figure 5) to verify whether 15 ns of MD simulation allows obtaining reliable TLL solvated structures in this destructive solvent. The average RMS deformation values and the average distances G and M (Table 3) confirmed that the change in conformation of TLL between 10 and 40 ns is negligible and evidently the solvated structures between 11–15 ns of the MD simulation represent the equilibrated production phase of MD and are suitable for the docking studies.

Deformation of the polypeptide backbone conformation

The RMSDs of the TLL polypeptide amino acid residues' C^{α} atoms were calculated along the MD simulation trajectory for both structures (one solvated in benzene and the other in methanol, Figure 6.). This parameter characterizes the extent of the conformational change of the enzyme backbone. For both of the TLL solvation runs, the value of RMSD of the TLL polypeptide amino acid residues' C^{α} atoms (\approx 1.5 Å in benzene and \approx 2.0 Å in methanol) is under the limit of RMSD (equal to 3.0 Å) $^{[34,37]}$ that marks the degree of the enzyme deformation that may cause the loss of its catalytic activity. In the current case, an interesting result is the considerably large value determined for the RMSD divergence^[46] of the corresponding C^{α} atoms in methanol versus those of benzene that exceeds 2.5 Å at 4 ns and reaches the plateau of 2.7-2.9 Å at 11 ns of MD simulation. The large divergence of structures observed indicates high probability of significant alteration in the catalytic performance of TLL solvated in benzene versus methanol.

Importantly, in the case of solvation in methanol, an equilibrated phase of the simulation between 10–40 ns can be distinguished from the initial 10 ns (+2 ns) relaxation phase (Table 3) by the average RMSD values, whereas the RMSD of the C^{α} atoms in benzene remains slightly increasing even after 10 ns of the MD simulation, albeit the change is negligible. It

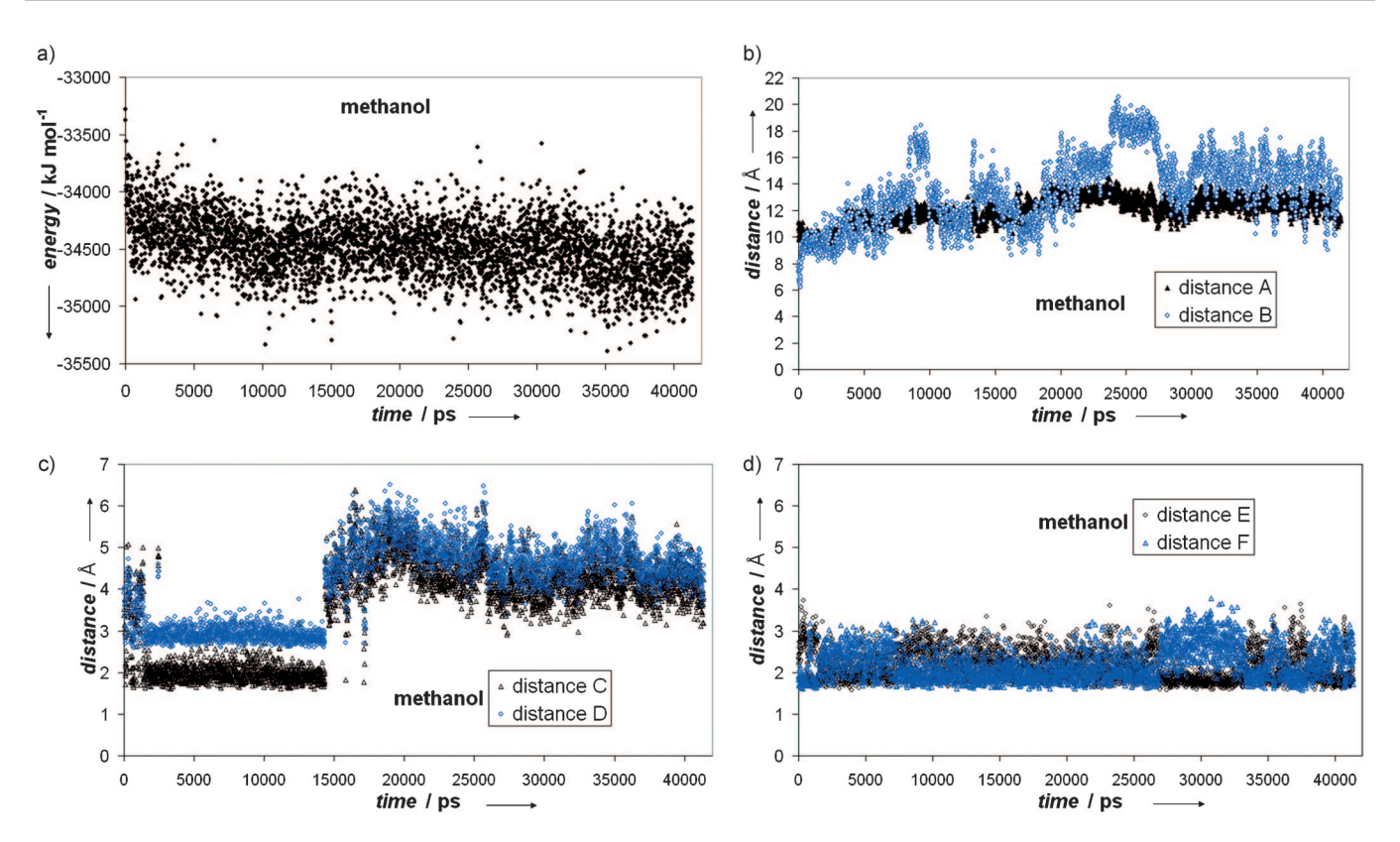


Figure 5. Evolution of the a) energy profile and b) interatomic distances A-D from MD simulation trajectory extended to 40.0 ns characterizing solvation of TLL in methanol.

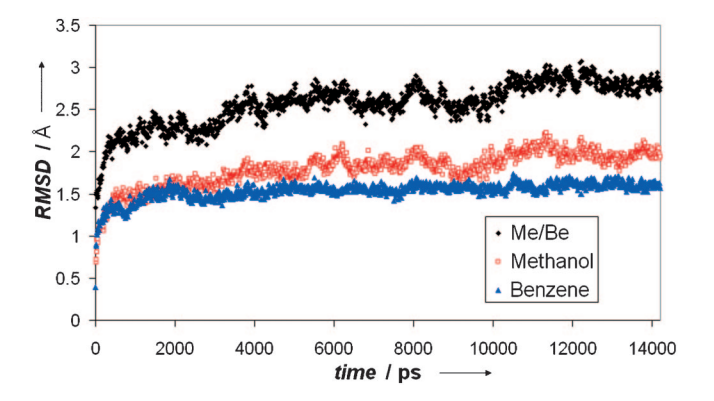


Figure 6. RMSD of backbone C^α atoms of TLL along the MD simulation trajectories in solvents methanol and benzene, respectively, and the divergence of the corresponding C^{α} atoms in methanol versus benzene (Me/Be).

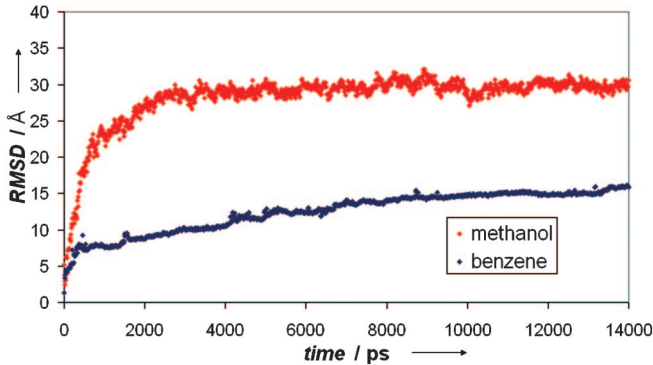


Figure 7. RMSD of enzyme-bound water molecules (relative to their starting positions at 0.0 ns) in MD simulation of TLL for solvation in methanol and benzene

should also be pointed out that for the solvation in benzene the catalytically important interatomic distances G and M, between 4 ns and 14 ns, behave in the manner characteristic to an equilibrated phase of the MD simulation as can be concluded by the close average values calculated for the different parts of the trajectory.

Repositioning of structural water

An important process to be explored, probably playing an important role in altering the catalytic performance of TLL in harsh methanol versus conservative benzene, is the repositioning of structural water molecules^[46,47] along the MD simulation trajectory. The loss of the catalytic activity of an enzyme is often associated with the dehydration of the protein structure by a water-miscible solvent. And conversely, solvents with higher log P are known to maintain the lipase activity in catalyzing acyl transfer reactions in these organic solvents.

To explore the hydration state along the MD simulation trajectory, the RMSD of enzyme-bound water molecules (relative to their starting positions at 0 ns) were calculated for MD solvation in methanol and benzene (Figure 7). The behavior of the structural water is completely different for TLL in methanol from that in benzene. In methanol, RMSD reach a plateau (30 Å) at approximately 4 ns of the MD simulation whereas in benzene the structural water is not removed from the enzyme to the bulk solvent phase and the value of RMSD is equal to 16 Å at 14 ns. The RMSD of the oxygen atoms of the water molecules from the corresponding starting points of MD simulation at 3, 7, 11, and 15 ns, which correspond to the docking structures (Table S1), was determined. By inspection of the RMSD values, it can be concluded that in methanol only 21 structural water molecules out of the total of 118 are not removed from the enzyme to the bulk solvent phase. In benzene medium, mobility of more than half of structural water molecules is very limited and, as mentioned above, structural water is not removed from the enzyme.

Docking analysis

Docking of 11 Ac-PGE₂ (1) was performed within a docking cell into the active site of TLL solvated structure from which the

solvent molecules had been eliminated. Each of the docking cells (Table S3) involves the constant set of the catalytically important amino acid residues, which are, therefore, geometrically unique for each of the docking structures. Average docking cell for the enzyme solvated in benzene is 115% by volume relative to TLL solvated in methanol. This difference is expectable because of the above conclusion that TLL solvated in benzene bears an open lid whereas in methanol the lid of TLL is closed.

Five solvated TLL structures were arbitrarily selected for docking studies from both of the MD solvations: from 3, 7, 11, and 15 ns, and also the minimum energy structure of MD simulation. The observed divergence of some MD characteristics, such as RMSD and interatomic distances (Tables 1 and 3) is the abovementioned reason behind the arbitrary choice of the multiple solvated structures.[48] In other words, we encountered complications in determining the duration of the inrelaxation/equilibration phase of the MD simulation and, therefore, it was decided to produce additional independent information about the MD simulation time necessary for the initial

relaxation of the lipase in the solvent box. This information was expected to be acquired by means of docking of the substrate into solvated structures taken from the different points of the MD simulation trajectory followed by the evaluation of the divergence of the results.

Alternate number of docking complexes (DC) was identified for different structures (Table S2). All DCs obtained were examined by 26 catalytically important interatomic distances. The full list of distances is presented in Table 4. Qualification criteria for productive DCs are as follows: the distances d₁, d₉ (the distance from Ser146 O^{γ} atom to C_1 of PG skeleton or to C_1 of 11acetyl group of the substrate, respectively) and d₁₇ or d₁₈ (the distance from His258 N^{τ} atom to (C₁₀)-H_{α} or to (C₁₀)-H_{β} hydrogen atom of the substrate, respectively) should be shorter than 4 Å and, in addition, for a qualifying DC at least one activating proton (to be donated for the hydrogen bonding) has to be closer than 3 Å to the accepting atom. All DCs obtained were carefully inspected and the complexes corresponding to

Table 4. List of the docking complex distances between the atoms of the potential reaction centers of the substrate 11 Ac-PGE₂ (1) and the catalytically important atoms of the amino acid residues of the active site of TLL pointing to three different catalytic reactions. The interatomic distance values found for two qualified probable docking complexes are presented.

Substrate atom specification ^[a]	Lipase atom specification ^[b]	Distance label; Type of action ^[c]		
1) Ester synthesis				
C ₁	Ser146-O ^y	d ₁ Nu	5.91	3.15
(C ₁)=O	Ser83-(O ^y)-H	d ₂ A	6.97	1.93
$(C_1) = O$	Ser83-(N)-H	d ₃ A	4.85	3.43
$(C_1) = O$	Leu147-(N)-H	d ₄ A	5.38	2.32
(C ₁) =O	Asn92-(N ^ω)-H	d₅ A	17.95	6.81
$(C_1) = O$	Asn92-(N ^ω)-H	d ₆ A	16.94	6.74
$(C_1) = O$	Asn92-(N)-H	d ₇ A	12.20	9.71
$(C_1) = O$	His145-(N ^π)-H	d ₈ A	10.09	7.55
2) Deacetylation				
C' ₁	Ser146-4-O ^y	d ₉ Nu	6.67	12.46
$(C'_1) = O$	Ser83-(O ^γ)-H	d ₁₀ A	4.19	11.85
$(C'_1) = O$	Ser83-(N)-H	d ₁₁ A	7.65	14.25
$(C'_1) = O$	Leu147-(N)-H	d ₁₂ A	8.84	13.30
$(C'_1) = O$	Asn92-(N ^ω)-H	d ₁₃ A	12.54	8.83
$(C'_1) = O$	Asn92-(N ^ω)-H	d ₁₄ A	11.30	7.34
$(C'_1) = O$	Asn92-(N)-H	d ₁₅ A	8.14	5.56
$(C'_1) = O$	His145-(N ^π)-H	d ₁₆ A	11.40	19.08
3) Elimination				
$(C_{10})-H_{\alpha}$	His258-N [™]	d ₁₇ B	3.84	13.11
(C ₁₀)-H _β	His258-N ^τ	d ₁₈ B	2.89	12.21
$(C_9) = O$	Ser83-(O ^γ)-H	d ₁₉ A	3.83	5.62
$(C_9) = O$	Ser83-(N)-H	d ₂₀ A	4.58	7.97
$(C_9) = O$	Ser146-(Ο ^γ)-Η	d ₂₁ A	4.02	8.57
$(C_9) = O$	Leu147-(N)-H	d ₂₂ A	2.43	7.25
$(C_9) = O$	His145-(N ^π)-H	d ₂₃ A	7.54	13.09
$(C_9) = O$	Asn92-(N ^ω)-H	d ₂₄ A	13.35	4.14
$(C_9) = O$	Asn92-(N ^ω)-H	d ₂₅ A	12.64	2.75
$(C_9) = O$	Asn92-(N)-H	d ₂₆ A	8.35	4.60
$(C'_1) = O$	His145-(N ^π)-H	d ₁₆ A	11.40	19.08
Binding energy of th	e docking complex (kcal mol ⁻¹)	9.51	7.63

[a] The numbering of the atoms of the substrate is depicted in Scheme 1; [a,b] the distances are measured between these atoms that are not in parentheses; [c] Nu, nucleophile; A, acid; B, base. [d] Determined for the more probable qualified docking complexes. [e] TLL structure11 ns, ranking of the complex=No. 4. [f] TLL structure = 11 ns, ranking of the complex = No. 5

Table 5. The qualified docking complexes. Binding energies and catalytically important interatomic distances (Table 4) that meet the qualification criteria for productive docking complexes^(a) suggesting occurrence of any of the three lipase-catalyzed methanolysis reactions of 11 Ac-PGE2 (1): esterification, deacetylation or elimination.

Docking medium	Docking structure min. E	Reaction type suggested by geometry of the docking corinteratomic distances $[\mathring{A}]$; binding energy $[kcal mol^{-1}]$; ranking Elimination Deacetylation						ing of the DC	•		
CH₃OH		d ₁₈ 2.52 (d ₂₁ 2.00, d ₂₀ 2.78)	4.47	10	d ₉ 2.94 (d ₁₁ 2.00)	3.13	13				
		20 /			d ₉ 3.12 (d ₁₀ 1.95)	6.44	03				
					d ₉ 3.94 (d ₁₃ 1.68, d ₁₀ 1.91)	6.77	02				
	3.0 ns	d ₁₈ 2.92 (d ₁₉ 2.11)	7.23	07							
	7.0 ns	d ₁₈ 3.65 (d ₂₂ 2.28)	8.5	09	d ₉ 3.96 (d ₁₁ 2.76)	8.47	10				
	11.0 ns	d ₁₈ 2.89 (d ₂₂ 2.43)	9.51	04							
	15.0 ns										
C ₆ H ₆	min. E	d ₁₈ 3.58 (d ₂₁ 2.30)	5.95	11				d ₁ 3.45 (d ₈ 2.77)	4.61	14	
								d ₁ 3.65 (d ₂ 2.29, d ₅ 2.95)	4.87	12	
	3.0 ns	d ₁₇ 3.94 (d ₂₀ 2.17, d ₁₉ 2.31, d ₂₂ 2.51)	7.08	17	d ₉ 2.76 (d ₁₀ 1.81, d ₁₁ 2.80, d ₁₂ 2.98)	7.8	07	d ₁ 2.72 (d ₂ 2.84)	8.15	05	
					d ₉ 3.29 (d ₁₀ 2.25)	7.47	10				
	7.0 ns				d ₉ 3.17 (d ₁₀ 2.29, d ₁₂ 2.92)	6.83	08	d ₁ 2.95 (d ₄ 1.95, d ₂ 2.11, d ₃ 2.26)	7.73	02	
					d ₉ 3.35 (d ₁₀ 1.87)	4.81	20	d ₁ 3.64 (d ₃ 2.33, d ₂ 2.80)	6.68	09	
	11.0 ns							d ₁ 3.15 (d ₂ 1.93, d ₄ 2.32)	7.63	05	
								d ₁ 3.25 (d ₃ 1.78)	5.65	18	
	15.0 ns				d ₉ 2.91 (d ₁₁ 1.94, d ₁₂ 2.19, d ₁₀ 2.58)	6.36	14	d ₁ 3.16 (d ₃ 2.68)	7.16	07	
					d ₉ 3.50 (d ₁₀ 2.07)	7.27	05	d ₁ 3.44 (d ₃ 1.79, d ₄ 2.75)	6.49	13	

[a] The qualification criteria for productive docking complexes are as follows: d1, d9, d17 or d18 < 4 Å (Table S4) and in addition to the previous criteria, at least one of the corresponding H bonds should be < 3 Å.

the qualification criteria are presented in Table 5, including the critical interatomic distances together with the binding energies and the rankings of the DCs.

The results presented in Table 5 demonstrate that none of the docking complexes obtained for TLL, solvated in methanol, suggest the catalysis of the esterification, and none of the docking complexes found for the TLL structures solvated in benzene for 7.0, 11.0, and 15.0 ns suggest the catalysis of the elimination for 11 Ac-PGE₂. It can be concluded from the undiverging results that the initial relaxation phase of MD for TLL in methanol is in essence probably over already to the 3.0 ns of MD simulation. However, notably the binding energy of the docking complexes, suggesting elimination, obtained for TLL solvated in methanol for 3.0, 7.0, and 11.0 ns is increasing, starting from 7.23 kcal mol⁻¹ for the DC of 3.0 ns TLL structure and attaining 8.5 and 9.51 kcal mol⁻¹ for DCs of 7.0 ns and of 11.0 ns TLL structures, respectively. Furthermore, the qualifying docking complexes found for the TLL MD structures solvated in benzene and in methanol for 11.0 ns of MD suggest that, depending on the solvent, only one reaction—esterification or elimination, respectively—is catalyzed; this is in exclusive accordance with the experiment.

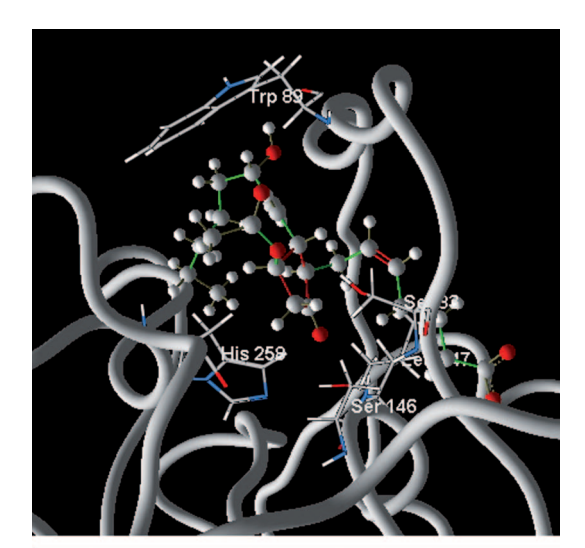
In conclusion, for the substrate 11 Ac-PGE₂, the esterification in benzene and the elimination in methanol, respectively, catalyzed by TLL can be considered the most probable reactions by the docking results. The deacetylation evidently should be the less favored and rather unprobable reaction to be catalyzed by TLL in both of the solvents, although it cannot be totally excluded by the docking results. However, deacetylated PGE₂ has not been detected by NMR in any of the products of TLL-catalyzed methanolysis of 11 Ac-PGE₂ obtained under different conditions (Scheme 2, Table 3).

The models of the most probable productive docking complexes are presented in Figure 8 in methanol: No. 4 (11.0 ns) and in benzene: No. 5 (11.0 ns). It can be seen that the bicyclic system of Trp89 covers the entrance of the active site of TLL in methanol, but in benzene it is repositioned away from the entrance. Also, depending on the solvent, a difference in position of the oxyanion hole can clearly be noted: Ser83 of TLL is removed from Ser146 of the catalytic triad in benzene relative to the position in methanol. Ser83 is a constituent part of the wing-type gate^[48b] helix of TLL (the lid).

By inspection of the models and taking into account the experimental results, it has to be concluded that the active site of TLL is accessible to the substrate 11 Ac-PGE₂ molecules in both solvents. In methanol, the size of the TLL active site is smaller than in benzene and the catalytic triad is situated close to the oxyanion hole. Such positioning explains why DCs with

$$\begin{array}{c} \begin{array}{c} RML & Run \ 2 \\ TLL & Run \ 3 \\ \hline 95\% \ CD_3OD \\ 5\% \ C_6D_6 \end{array} \\ \begin{array}{c} CALB & Run \ 4 \\ \hline 95\% \ CD_3OD \\ 5\% \ C_6D_6 \end{array} \\ \end{array}$$

Scheme 2. Lipase-catalyzed methanolysis of 11 Ac-PGE₂ (1) by varying the catalyst or the reaction medium. The alternative potential reaction centers RC1, RC2, and RC3 in the substrates as well as the centers actually attacked in the products are labeled.



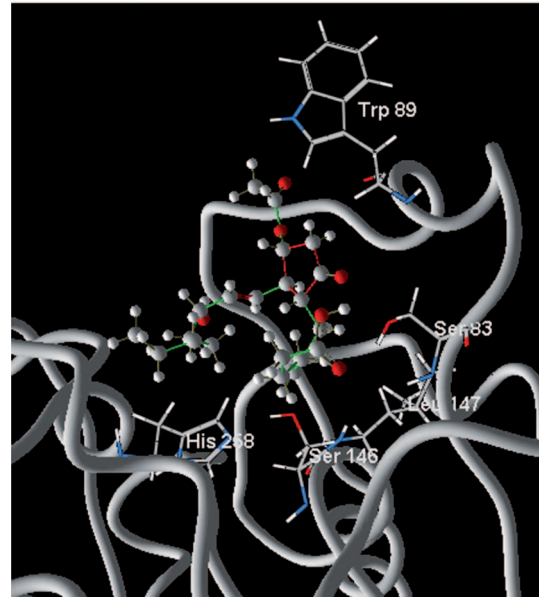


Figure 8. The most probable productive docking complexes a) in methanol, No. 4 (11.0 ns) and b) in benzene, No. 5 (11.0 ns). For the interatomic distances, see Figure 9 and Table 4.

the orientation that could refer to the esterification of the substrate molecule cannot form. The observation that none of the DCs referring to the elimination (for 7, 11, and 15 ns) are formed in the active site of TLL solvated in benzene, despite the fact that there are no obvious spatial restrictions, seems intriguing.

The schemes of the most probable productive docking complexes of 11 Ac-PGE2 in TLL (11 ns structures) solvated in methanol and benzene, respectively, are presented in Figure 9 and suggest elimination and esterification, respectively.

Experimental exploration of the catalytic performance of the lipases

Samples of 11 Ac-PGE₂ (1) were incubated with TLL, Rhizomucor miehei lipase (RML), and Candida antarctica lipase B (CALB), and without the enzymes, respectively, in CD₃OD/C₆D₆ (95/5) and analyzed by NMR spectroscopy (Scheme 2, Table 6). [49] TLL and its close structural counterpart Rhizomucor miehei lipase catalyzed the prompt elimination that occurs exclusively; no other reaction was observed.

The spontaneous elimination observed in the reference trial without enzyme was negligible (Table 6, run 1). Catalytic performance of elimination was observed also for CALB, which bears a very different lid from that of TLL and RML. The lid of CALB is considered to be, independently of the solvent, relatively open, and as a result, CALB also catalyzed nonselectively esterification and deacetylation, albeit at a low rate. TLL in CH₃OH/C₆D₆ (5/95) medium catalyzed selectively ester synthesis, but the reaction rate was much lower than was estimated for TLL-catalyzed elimination (Table 6).

Conclusions

To explain the switch of reactions in methanolysis of 11-acetylprostaglandin E2 (11 Ac-PGE2, 1) catalyzed by Thermomyces lanuginosus lipase (TLL), dependent on the methanol concentration in the reaction medium, molecular dynamics (MD) simula-

Figure 9. The docking complexes of substrate 1 in the active site of TLL. A2) Docking complex no. 4 of the docking structure from 11 ns of the TLL MD simulation in methanol. Probable elimination mechanism via the enolate is depicted by electron-pushing arrows. The distances (Å) between atoms are indicated by dotted lines. B2) Docking complex no. 5 of the docking structure from 11 ns of the TLL MD simulation in benzene. This docking complex suggests esterification of the substrate. The distances between atoms are indicated with dotted lines.

tions of the solvation of TLL in two solvents, benzene and methanol were performed, respectively, by using force field AMBER 99. The solvated enzyme structures were used for docking calculations from the following arbitrarily chosen points on the MD simulation trajectory: 3.0 ns, 7.0 ns, 11.0 ns, 15.0 ns, and additionally the minimum energy structures were chosen from both of the solvations. A docking analysis (using Autodock 4.0 software) of the substrate 11 Ac-PGE2 into the TLL active site was performed within the docking cell that involves catalytically important amino acid residues of the catalytic triad, the oxyanion hole, and the lid of the active site. The docking poses obtained were analyzed by the qualification criteria (based on interatomic distances) to suggest the occurrence of any of the three reactions: esterification, deacetylation, or elimination. An overall evaluation of the docking poses found for all docking structures clearly suggested the catalysis of esterification in benzene and elimination in methanol, respectively. The docking poses found for solvated TLL structures taken at 11.0 ns of both of the MD solvations exclusively suggested the reaction that matches with the experimental results: the catalysis of esterification for benzene-solvated TLL and elimination for methanol-solvated enzyme. The TLL-solvated structures corresponding to the minimum energy on the MD simulation trajectories did not afford docking results matching with the experiment and their use cannot be recommended. The switch of the catalytic performance of TLL dependent on the methanol concentration in the reaction medium can be explained by the closing of the lid and a shift of the oxyanion hole towards Ser146 of the catalytic triad in methanol. As a result, the O^{γ} atom of Ser146 becomes tightly H-bonded by the oxyanion hole Ser83 NH hydrogen atom, and its nucleophilicity is strongly reduced. Concurrently, Ser83 NH and OH hydrogen atoms of the oxyanion hole are repositioned to a catalytically proper distance (4–5 Å) to N^τ of His258, in this way probably enabling the TLL to act as an acetyl-β-ketol eliminase. A very different behavior of RMSD of the structural water molecules along the MD trajectory depending on the solvent should be stressed.

Experimental Section

Molecular modeling methodology

A modeling study starting from MD simulation of TLL in two solvent boxes for solvation of the enzyme in neat methanol as well as in neat benzene instead of the 95/5 and 5/95 solvent mixtures (used in synthetic trials) was undertaken. The final results of the work indicate that this simplification was valid.

Table 6. (1).	. The enzym	e-substrate s	ystems investi	gated and th	e results of NMR spectrosco	opic monitoring	of the lipase	e-catalyzed m	ethanolysis of 11 Ac-PGE ₂
Run	Sub	strate	Enzy pre		Reaction medium ^[a] (vol./vol.)	Reaction Time		ducts med	Initial velocity of the main reaction
	No.	[mg]	lipase	[mg]		[h]	No.	[%] ^[b]	$[\mu mol mL^{-1} h^{-1}]^{[c]}$
1	1	10	_	_	CD ₃ OD/C ₆ D ₆ (95/5)	42	3	1	0.007
2	1	10	RML	70	CD ₃ OD/C ₆ D ₆ (95/5)	19	3	35	6.97
3	1	10	TLL	100	CD ₃ OD/C ₆ D ₆ (95/5)	47	3	59	5.61
4	1	10	CALB	60	CD ₃ OD/C ₆ D ₆ (95/5)	103	3	17	0.56
							4	< 5	
							2	< 5	
5	1	10	TLL	100	CH ₃ OH/C ₆ D ₆ (5/95)	139	2	54	1.22

[a] Reaction volume was 1.0 mL for all runs. [b] Conversion rate determined by NMR analysis. [c] Estimated initial velocity per 1 g of immobilized enzyme preparation (based on conversion rates determined by NMR).

Molecular mechanics and MD calculations were performed with the software package YASARA^[50,51] in which AMBER99 force field was used. MD simulation methodology was used to generate TLL structures solvated in benzene and in methanol. The geometries of solvated TLL obtained were used in studies of the substrate docking. The influence of the two solvents was studied also in comparison with the in vacuo MD simulation results. The structures obtained in these three media are characterized by distances between the catalytically important atoms of the catalytic triad, the oxyanion hole, and the lid of the enzyme, as well as by energies of the systems and RMSD of the lid and also by RMSD of structural water and the backbone of the whole enzyme. The docking of the substrate 11 Ac-PGE₂ (1) to several TLL structures corresponding to the geometries of the solvated enzyme taken from the MD simulation trajectory points was performed. Identification of probable productive binding modes and sites of the above substrate in the active site of TLL was performed.

The TLL crystal structure was taken from the Protein Data Bank (PDB entry: 1DTE; with the resolution of 2.35 Å). This structure contains two chains, both of which are composed of 269 amino acids. Only one protein chain with its 118 structural water molecules was kept and used for modeling. The remaining part of the protein was removed.

The following modeling steps were performed: Firstly, the hydrogen atoms were added to the protein structure. Secondly, a three stage structure relaxation and energy minimization procedure for the protein was performed. In the first stage, only the hydrogen atoms were minimized; in the second stage, the conformation of the backbone was also minimized; and in the third stage, the energy of the entire system was minimized. A rectangular simulation cell around all atoms of TLL was created and subsequently extended by 5 Å beyond the outer boundary of atoms (an appropriate parameter: extension = 5 Å was used).

Reaction medium: To mimic the influence of solvent during subsequent MD runs, the simulation cell was "filled" with the desired solvent in such a way that the solvent density fulfilled the following density values: 0.87 g mL⁻¹ for benzene and 0.79 g mL⁻¹ for methanol. In this way 1028 benzene and 2261 methanol molecules appeared in the corresponding simulation cell, respectively.

An MD simulation was allowed to run for the above prepared enzyme within the time interval of 2000 ps for preliminary optimization of the solvated structure. The force field was AMBER99^[52,53] with a cutoff value of 7.86 Å for the van der Waals forces; for the long range electrostatics the Particle Mesh Ewald approach^[54] was used. The simulation was run under periodic boundary conditions, and at 298 K temperature and 1.0 atm. of pressure.

Multiple time steps were used: 1.25 fs for intramolecular and 2× 1.25 fs for intermolecular forces. After each 10 ps all the coordinates of the complex were saved as a snapshot. MD simulation results were prevailingly analyzed with the help of YASARA software. However, part of the trajectory analysis was performed with the VMD molecular visualization and analysis package that was deemed more suitable in certain cases.

The following snapshots were selected: the first four were from 3.0, 7.0, 11.0, 15.0 ns of the MD simulation trajectory and the fifth structure corresponded to the minimum of the potential energy from the MD simulation trajectory for subsequent docking calculation. Subsequently, each of the previously selected solvated TLL structures was energy-minimized and solvent molecules were removed from the system.

Neutralization: YASARA predicts pK_a values for Asp, Glu, His, and Lys residues using a method that has been calibrated on experimental pK_a measurements. Based on the chosen pH 7, YASARA assigns the protonation states and overall charges to the amino acids. The charges were assigned as follows: Asp, Glu (-1); Lys, Arg (+1); His, Cys, and Tyr (0).

Docking calculation: The docking of solvated TLL with the substrate 11 Ac-PGE₂ (1) was performed with the YASARA program, which has a fully integrated and customized version of Autodock $4.0.^{\tiny{[55]}}$ The docking target structures were taken, as mentioned above, from the MD simulation trajectory at: 3.0, 7.0, 11.0, and 15.0 ns and additionally, the solvated structure of minimum potential energy was also taken. We chose 250 docking runs for the search for preferable binding sites and modes of 11 Ac-PGE₂ (1) to a solvated, energy minimized and afterwards fixed structure of TLL. The search was started from a random location of the substrate within the simulation cell as well as from a loose substrate conformation, that is, by using a global docking method. Thus, conformational flexibility was taken into account, that is, by allowing rotation around the dihedrals during the docking runs. The docking cells were selected to include the substrate molecule and all atoms of the residues of Asp201, His258, Ser146, Ser83, Leu147, Asn92, His145, and Trp89. The sizes of the docking cells are presented in Table S3.

Experimental

Materials: Deuterated solvents: [D₄]MeOH, 99.8 atom % D (Aldrich); [D₆]benzene, 99.6 atom% D (ISOTEC). Immobilized enzymes were donated by the producer: T. lanuginosus lipase (LIPOLASE 100 T; Batch no.: LA9 0148103; Novo Nordisk A/S); Rhizomucor miehei lipase (RML, Lipozyme RM IM; batch no.: LUX00205; Novozymes); Candida antarctica lipase B (CALB, Novozym 435; batch no.: LC200210; Novozymes). Prostaglandins: the substrate 11-acetylprostaglandin E₂ (1) and the standards of the products, PGA₂ (3), PGE₂, and 11-acetyl-prostaglandin E₂ methyl ester (2) were purchased from Kevelt Ltd. (Tallinn); all of these prostanoids were characterized by ¹H and ¹³C NMR spectra and microanalyses data. Thin layer chromatography was performed using TLC Silica gel 60 F254 aluminum sheets (Merck); compounds were visualized using anisaldehyde/EtOH/H₂SO₄ solution.

Methods: ¹H and ¹³C NMR spectra were recorded on a Bruker Avance 800 MHz spectrometer. All signals were referenced in relation to the solvent signal. 2D Fourier transform methods were used for the full assignment of NMR spectra. The details of the different methanolysis runs of 11 Ac-PGE₂ (1) are presented in Table 3.

Protocol of the lipase-catalyzed methanolysis: The sample of 11 Ac-PGE₂ (10 mg; 25 μmol) was dissolved in the solvent mixture (1 mL). Immobilized enzyme was added, and the mixture was shaken at RT until a suitable conversion was identified by using TLC. The reaction solution was introduced into a NMR tube (5 mm) and the NMR spectra (¹H and ¹³C) were recorded (NMR analysis was repeated up to four times). Elimination and esterification was monitored by characteristic signals: 6.14 and 3.65 ppm, which correspond to (C₁₀)-H of PGA₂ and H atoms of the methoxy group of the ester, respectively. The integral intensities determined were standardized against an integrated signal (at 0.85 ppm) of hydrogen atoms of the terminal methyl group of the PG molecule. The initial velocities estimated are presented in Table 3. Identification of the minor products and estimation of their content were based on both, the inspection of the NMR data, as well as on TLC analysis using standards.

Acknowledgements

The authors are grateful to Ms. Mae Parve for helpful discussions. We thank the Archimedes Foundation (project no. 3.2.0501.10-0004), Tallinn University of Technology (grant B35), Estonian Ministry of Education and Research (project no. SF0140133s08, SF0180073s08, SF0690034s09, SF140010s08, ETF 8880, ETF 7009) and Estonian Research Agency Grant IUT19-9 for financial support.

Keywords: elimination · enzyme catalysis · molecular dynamics · prostaglandins · solvent effects

- [1] S. Das, S. Chandrasekhar, J. S. Yadav, R. Grée, Chem. Rev. 2007, 107, 3286 - 3337.
- [2] A. J. Weinheimer, R. L. Spraggins, Tetrahedron Lett. 1969, 10, 5185-5188.
- [3] W. P. Schneider, R. D. Hamilton, L. E. Rhuland, J. Am. Chem. Soc. 1972, 94, 2122-2123.
- [4] K. Valmsen, I. Järving, W. E. Boeglin, K. Varvas, R. Koljak, T. Pehk, A. R. Brash, N. Samel, Proc. Natl. Acad. Sci. USA 2001, 98, 7700 - 7705.
- [5] A. I. Hubich, A. Y. Bondar, T. U. Kastsiuk, U. A. Kastsiuk, F. A. Lakhvich, M. V. Sholukh, Hepatology Res. 2007, 37, 416-424.
- [6] Y. Kikuchi, T. Kita, J. Hirata, M. Fukushima, Cancer Metastasis Rev. 1994, 13, 309 - 315.
- [7] S. Gharbi, B. Garzón, J. Gayarre, J. Timms, D. Pérez-Sala, J. Mass Spectrom. 2007, 42, 1474-1484.
- [8] H.-L. Zhang, Z.-L. Gu, S. I. Savitz, F. Han, K. Fukunaga, Z.-H. Qin, J. Neurosci. Res. 2008, 86, 1132-1141.
- [9] X.-H. Xu, H.-L. Zhang, R. Han, Z.-L. Gu, Z.-H. Qin, Brain Res. 2006, 1102, 154-162.
- [10] M. Gorospe, N. J. Holbrook, Cancer Res. 1996, 56, 475-479.
- [11] H. Sasaki, M. Fukushima, Anticancer Drugs 1994, 5, 131-138.
- [12] M. G. Santoro, A. Crisari, A. Benedeto, C. Amici, Cancer Res. 1986, 46, 6073 - 6077.
- [13] A. S. Ratnayake, T. S. Bugni, C. A. Veltri, J. J. Shalicky, C. M. Ireland, Org. Lett. 2006, 8, 2171-2174.
- [14] I. Vallikivi, I. Järving, T. Pehk, N. Samel, V. Tõugu, O. Parve, J. Mol. Catal. B 2004, 32, 15-19.
- [15] O. Parve, I. Järving, I. Martin, A. Metsala, I. Vallikivi, M. Aidnik, T. Pehk, N. Samel, Bioorg. Med. Chem. Lett. 1999, 9, 1853 - 1858.
- [16] I. Vallikivi, Ü. Lille, A. Lookene, A. Metsala, P. Sikk, V. Tõugu, H. Vija, L. Villo, O. Parve, J. Mol. Catal. B 2003, 22, 279-298.
- [17] D. F. Taber, K. Kanai, Tetrahedron 1998, 54, 11767 11782.
- [18] D. F. Taber, M. Xu, J. C. Hartnett, J. Am. Chem. Soc. 2002, 124, 13121-
- [19] D. F. Taber, K. Kanai, R. Pina, J. Am. Chem. Soc. 1999, 121, 7773-7777.
- [20] D. F. Taber, Q. Jiang, J. Org. Chem. 2001, 66, 1876 1884.
- [21] M. Holmquist, Curr. Protein Peptide Sci. 2000, 1, 209-235.
- [22] V. Ferrario, C. Ebert, L. Knapic, D. Fattor, A. Basso, P. Spizzo, L. Gardossi, Adv. Synth. Catal. 2011, 353, 2466-2480.
- [23] S. Santini, J. M. Crowet, A. Thomas, M. Paquot, M. Vandenbol, P. Thonart, J. P. Wathelet, C. Blecker, G. Lognay, R. Brasseur, L. Lins, B. Charloteaux, Biophys. J. 2009, 96, 4814-4825.
- [24] S. Rehm, P. Trodler, J. Pleiss, Protein Sci. 2010, 19, 2122-2130.
- [25] A. Salis, I. Svensson, M. Monduzzi, V. Solinas, P. Adlercreutz, Biochim. Biophys. Acta Proteins Proteomics 2003, 1646, 145-151.
- [26] F. Secundo, G. Carrea, J. Mol. Catal. B 2002, 782, 1 10.

- [27] P. Virsu, A. Liljeblad, A. Kanerva, L. T. Kanerva, Tetrahedron: Asymmetry **2001**, 12, 2447 - 2455.
- [28] Y. Shimada, Y. Watanabe, A. Sugihara, Y. Tominaga, J. Mol. Catal. B 2002, 17. 133 - 142.
- [29] J. Lu, L. Deng, R. Zhao, R. Zhang, F. Wang, T. Tan, J. Mol. Catal. B 2010, *62*, 15 – 18,
- [30] A. Bajaj, P. Lohan, P. N. Jha, R. Mehrotra, J. Mol. Catal. B 2010, 62, 9-14.
- [31] K. Nie, F. Xie, F. Wang, T. Tan, J. Mol. Catal. B 2006, 43, 142-147.
- [32] C. Branneby, P. Carlquist, A. Magnusson, K. Hult, T. Brinck, P. Berglund, J. Am. Chem. Soc. 2003, 125, 874-875.
- [33] L. Villo, A. Metsala, O. Parve, T. Pehk, Tetrahedron Lett. 2002, 43, 3203-3207.
- [34] P. Berglund, I. Vallikivi, L. Fransson, H. Dannacher, M. Holmquist, M. Martinelle, F. Björkling, O. Parve, K. Hult, Tetrahedron: Asymmetry 1999, 10, 4191 - 4202
- [35] I. Vallikivi, L. Fransson, K. Hult, I. Järving, T. Pehk, N. Samel, V. Tõugu, L. Villo, O. Parve, J. Mol. Catal. B 2005, 35, 62-69.
- [36] S. Raza, L. Fransson, K. Hult, Protein Sci. 2001, 10, 329-338.
- [37] E. B. De Oliveira, C. Humeau, L. Chebil, E. R. Maia, F. Dehez, B. Maigret, M. Ghoul, J.-M. Engasser, J. Mol. Catal. B 2009, 59, 96 - 105.
- [38] P. Trodler, J. Pleiss, BMC Struct. Biol. 2008, 8:9 (DOI: 10.1186/1472-6807-
- [39] C. Li, T. Tan, H. Zhang, W. Feng, J. Biol. Chem. 2010, 285, 28434-28441.
- [40] M. Norin, F. Haeffner, K. Hult, O. Edholm, Biophys. J. 1994, 67, 548-559.
- [41] B. A. Tejo, A. B. Salleh, J. Pleiss, J. Mol. Model. 2004, 10, 358-366.
- [42] M. Norin, F. Haeffner, A. Achour, T. Norin, K. Hult, Protein Sci. 1994, 3, 1493 - 1503.
- [43] I. J. Colton, S. N. Ahmed, R. J. Kazlauskas, J. Org. Chem. 1995, 60, 212-217
- [44] a) M. W. van der Kamp, R. Chaudret, A. J. Mulholland, FEBS J. 2013, 280, 3120-3131; b) H. Park, K. M. Merz, J. Am. Chem. Soc. 2003, 125, 901-
- [45] C. Kanchanabanca, W. Tao, H. Hong, Y. Liu, F. Hahn, M. Samborskyy, Z. Deng, Y. Sun, P. F. Leadlay, Angew. Chem. Int. Ed. 2013, 52, 5785-5788; Angew. Chem. 2013, 125, 5897 – 5900.
- [46] L. Yang, J. S. Dordick, S. Garde, Biophys. J. 2004, 87, 812-821.
- [47] L. A. S. Gorman, J. S. Dordick, Biotechnol. Bioeng. 1992, 39, 392 397.
- [48] a) T. D. Romo, A. Grossfield, J. Chem. Theory Comput. 2011, 7, 2464-2472; b) A. Gora, J. Brezovsky, J. Damborsky, Chem. Rev. 2013, 113, 5871 - 5923.
- [49] a) H. K. Weber, H. Weber, R. J. Kazlauskas, Tetrahedron: Asymmetry 1999, 10, 2635-2638; b) H. Weber, L. Brecker, Curr. Opin. Biotechnol. 2000, 11, 572 – 578; c) H. Weber, L. Brecker, D. De Souza, H. Griengl, D. W. Ribbons, H. K. Weber, J. Mol. Catal. B 2002, 19/20, 149-157.
- [50] S. B. Nabuurs, M. Wagener, J. De Vlieg, J. Med. Chem. 2007, 50, 6507 -
- [51] a) E. Krieger, T. Darden, S. Nabuurs, A. Finkelstein, G. Vriend, *Proteins* Struct. Funct. Bioinf. 2004, 57, 678-683; b) www.yasara.org, Ver. 10.3.21.
- [52] J. Wang, P. Cieplak, P. A. Kollman, J. Comput. Chem. 2000, 21, 1049-
- [53] Y. Duan, C. Wu, S. Chowdhury, M. C. Lee, G. Xiong, W. Zhang, R. Yang, P. Cieplak, R. Luo, T. Lee, J. Comput. Chem. 2003, 24, 1999-2012.
- [54] U. Essmann, L. Perera, M. L. Berkowitz, T. Darden, H. Lee, L. G. Pedersen, J. Chem. Phys. B 1995, 103, 8577-8593.
- [55] G. M. Morris, D. S. Goodsell, R. S. Halliday, R. Huey, W. E. Hart, R. K. Belew, A. J. Olson, J. Comput. Chem. 1998, 19, 1639-1662.

Received: January 8, 2014 Revised: April 1, 2014

Published online on June 20, 2014